Structure of an EF-Tu Complex with a Thiazolyl Peptide Antibiotic Determined at 2.35 Å Resolution: Atomic Basis for GE2270A Inhibition of EF-Tu[†,‡]

Susan E. Heffron and Frances Jurnak*

Department of Physiology and Biophysics, 346-D Med Sci I, University of California, Irvine, California 92697-4560

Received June 15, 1999; Revised Manuscript Received October 7, 1999

ABSTRACT: The structure of a 1:1 molar complex between *Escherichia coli* elongation factor (EF) Tu-GDP and the cyclic thiazolyl peptide antibiotic, GE2270A, has been determined by X-ray diffraction analysis to a resolution of 2.35 Å and refined to a crystallographic refinement factor of 20.6%. The antibiotic binds in the second domain of EF-Tu-GDP, making contact with three segments of amino acids (residues 215−230, 256−264, and 273−277). The majority of the protein−antibiotic contacts are van der Waals interactions. A striking feature of the antibiotic binding site is the presence of a salt bridge, not previously observed in other EF-Tu complexes. The ionic interaction between Arg 223 and Glu 259 forms over the antibiotic and probably accounts for the strong affinity observed between EF-Tu and GE2270A. Arg 223 and Glu 259 are highly conserved, but not invariant throughout the prokaryotic EF-Tu family, suggesting that the antibiotic may bind EF-Tu from some organisms better than others may. Superposition of the antibiotic binding site on the EF-Tu-GTP conformation reveals that one region of the antibiotic would form steric clashes with the guanine nucleotide-binding domain in the GTP, but not the GDP, conformation. Another region of the antibiotic binds to the same site as the aminoacyl group of tRNA. Together with prior biochemical studies, the structural findings confirm that GE2270A inhibits protein synthesis by blocking the GDP to GTP conformational change and by directly competing with aminoacyl-tRNA for the same binding site on EF-Tu. In each of the bacterial strains that are resistant to GE2270A, the effect of a site-specific mutation in EF-Tu could explain resistance. Comparison of the GE2270A site in EF-Tu with sequence homologues, EF-G and EF-1α, suggests steric clashes that would prevent the antibiotic from binding to translocation factors or to the eukaryotic equivalent of EF-Tu. Although GE2270A is a potent antibiotic, its clinical efficacy is limited by its low aqueous solubility. The results presented here provide the details necessary to enhance the solubility of GE2270A without disrupting its inhibitory properties.

EF-Tu[1] is an essential component in the bacterial protein biosynthetic pathway. Its primary function is to recognize and transport noninitiator aminoacyl-tRNAs to the A site of mRNA-programmed ribosomes during the elongation cycle (*1*). During protein synthesis, EF-Tu undergoes a series of conformational changes as it interacts with GDP, GTP, EF-Ts, and aminoacyl-tRNA. Crystallographic studies of four EF-Tu complexes not only have identified the binding sites of the cellular components but also have led to a detailed knowledge of the dramatic conformational changes that occur upon the exchange of guanine nucleotides (*2*−*7*). Two major classes of antibiotics are known to interact directly with EF-Tu and inhibit its function in one or more steps of the elongation cycle. Antibiotics belonging to the cyclic thiazolyl peptide class inhibit protein synthesis by blocking formation of the EF-Tu-GTP−aminoacyl-tRNA complex (*8*−*10*). Antibiotics of the kirromycin family inhibit protein synthesis by preventing the release of EF-Tu from the ribosome following GTP hydrolysis (*11*, *12*). In addition, several other antibiotics, including pulvomycin (*13*) and enacyloxin IIa (*14*), have been reported to interact with EF-Tu and interfere with different steps in the elongation cycle. To further understand the inhibition of protein synthesis at the atomic level, the structure of *Escherichia coli* EF-Tu-GDP in complex with a cyclic thiazolyl peptide antibiotic, GE2270A, has been determined by X-ray diffraction techniques and refined to a resolution of 2.35 Å.

GE2270A is a member of the cyclic thiazolyl peptide family that inhibits bacterial protein synthesis (*15*). Other members that share a similar cyclic thiazolyl peptide skeleton include GE37468 (*16*), the amythiamicins (*10*), thiostrepton (*17*), nosiheptide (*18*), siomycin, and micrococcin (*19*). The first two antibiotics interact directly on EF-Tu, and the latter four antibiotics appear to act by interacting directly with the

[†] This work was supported by NIH Grant GM26895 to F.J.

[‡] Atomic coordinates have been deposited with the Research Collaboratory for Structural Bioinformatics (RCSB) Protein Data Bank (file 1D8T).

* Corresponding author. Phone: (949) 824-6623. Fax: (949) 824-8540. E-mail: jurnak@uci.edu. Member, Chao Family Comprehensive Cancer Center, University of California, Irvine.

[1] Abbreviations: EF, elongation factor; EF-Tu, elongation transfer factor; EF-G, elongation translocation factor; EF-Ts, nucleotide-exchange elongation factor; GDP, guanine nucleotide diphosphate; GTP, guanine nucleotide triphosphate; MIC, minimum inhibitory concentration; S/N, signal-to-noise ratio; F_o, observed structure factor amplitude; F_c, calculated structure factor amplitude; R_{work}, crystallographic refinement factor calculated with 93% of the data; R_{free}, crystallographic refinement factor calculated with 7% of the data selected at random; σ, one standard deviation; NMR, nuclear magnetic resonance.

10.1021/bi9913597 CCC: $19.00
Published on Web 12/08/1999

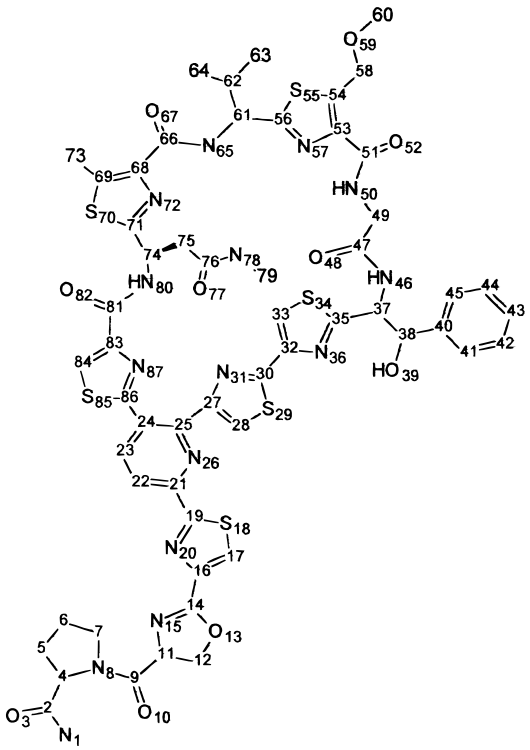

FIGURE 1: Schematic of GE2270A. Nitrogen, oxygen, and sulfur atoms are specifically indicated, but carbon atoms are assumed. The numbers indicate those assigned to the atomic model.

ribosome (*20*, *21*). Thiostrepton is the best-characterized member and is known to interact with the 23S rRNA region, encompassing nucleotides 1052−1112 (*22*). This same region is believed to be one of several sites of interaction with translocation factor, EF-G, and is near to but not part of the EF-Tu binding site on the ribosome. The chemical structure of GE2270A and the nomenclature used herein are presented in Figure 1. GE2270A is produced by *Planobispora rosea*, a microorganism that produces an EF-Tu variant that does not bind to the inhibitor (*23*, *24*). Interest in GE2270A has been motivated by the observations that the antibiotic has MIC values ranging from 0.01 to 1.00 μg/mL against anaerobic microorganisms and Gram-positive bacteria, including staphylococci and enterococci isolates resistant to ampicillin, methicillin, erythromycin, glycopeptides, and gentamicin (*15*, *25*). In addition to *P. rosea*, the only other known resistance to GE2270A occurs in *Bacillus subtilis* strains specifically selected for resistance to GE2270A (*23*, *26*). Although GE2270A is an effective inhibitor of prokaryotic protein synthesis in vitro, its utility as an antibiotic has been limited by its low solubility in aqueous solutions. The three-dimensional structure of EF-Tu-GDP−GE2270A suggests how the antibiotic may be improved to increase its solubility.

GE2270A interacts in a 1:1 molar complex with EF-Tu with such high affinity that denaturation of the protein is required to release the antibiotic. The binding of GE2270A to EF-Tu is readily detected by a mobility shift of the protein in an electric field, an observation that suggests GE2270A alters the surface charge of the protein (*8*, *27*). Several biochemical studies have indicated that GE2270A affects the properties of EF-Tu-GTP, but not those of EF-Tu-GDP. GE2270A also impairs the binding of aminoacyl-tRNA to EF-Tu-GTP (*8*, *9*, *27*). However, the biochemical studies have not clearly established whether GE2270A competes directly for the tRNA binding site or blocks the change to the GTP conformation that is required for the formation of the aminoacyl-tRNA binding pocket on EF-Tu. Superposition of the GE2270A binding site onto each of the EF-Tu conformational states provides a clear explanation for the observed biochemical properties and its mode of inhibition. Further analysis also demonstrates that GE2270A is unlikely to bind to structural homologues of EF-Tu, such as translocation factor EF-G and the eukaryotic elongation factor EF-1α.

EXPERIMENTAL PROCEDURES

Preparation and Crystallization of the EF-Tu-MgGDP−GE2270A Complex. EF-Tu-MgGDP (molecular weight of 43 643) was isolated from *E. coli* B cells as previously described (*28*). GE2270A (molecular weight of 1289) was obtained as a gift from Biosearch Italia (Gerenzano, Italy). Unless otherwise noted, all reagents were purchased from Sigma (St. Louis, MO), and all subsequent procedures were carried out under yellow light. A 50 mM stock of GE2270A was prepared by dissolving the antibiotic in dimethyl sulfoxide and stored at −80 °C in the dark. The EF-Tu-MgGDP−GE2270A complex was prepared by incubating GE2270A in a 1:1 molar ratio with EF-Tu-MgGDP in buffer A containing 50 mM Tris-HCl (pH 7.6), 10 mM $MgCl_2$, and 5×10^{-7} M GDP for 2 h. The mixture was then centrifuged to remove a white precipitate and dialyzed against buffer A for 24 h. For crystallization, 15 μL of the complex, at a concentration of 10.4 mg/mL, was mixed with 5 μL of 20% (w/v) polyethylene glycol 3350 (J. T. Baker, Phillipsburg, NJ) in 0.2 M ammonium acetate and 0.1 M ammonium citrate. The droplet was placed in a sitting drop crystallization box (Charles Supper Co., Natick, MA) over a reservoir containing 400 μL of 50% (w/v) polyethylene glycol 8000 and stored in the dark at 20 °C. Clusters of single crystals grew to maximum dimensions of 0.02 mm × 0.10 mm × 0.20 mm within 7 days.

Flash-Freezing, Data Collection, and Processing. A single crystal was cleaved from a cluster of crystals, captured on a nylon loop, and quickly passed through a 50% glycerol solution before being frozen in a stream of nitrogen at −178 °C. A complete X-ray diffraction data set was measured from a single crystal at Stanford Synchrotron Radiation Laboratory (SSRL) beamline 7-1 at 1.08 λ. The reflections were indexed, integrated, and scaled with MOSFLM (*29*, *30*) and SCALA (*31*). The frozen crystal had a diffraction symmetry consistent with space group *C*2 and the following unit cell parameters: $a = 133.47$ Å, $b = 45.17$ Å, $c = 144.00$ Å, and $\beta = 94.64°$. The diffraction space covered was complete to 86.9% at 2.35 Å, with 60.7% completeness in the 2.35−2.41 Å bin and 82.4% completeness in the 2.41−2.48 Å bin. The isotropic thermal factor was 29.8 Å^2, as determined by statistical analysis of the intensities with a Wilson plot calculated by TRUNCATE (*32*).

Molecular Replacement. The structure was determined by molecular replacement methods using the program X-PLOR (*33*), version 3.851. The search molecule consisted of chain A of the *E. coli* EF-Tu-MgGDP model, which included residues 9−393 of EF-Tu, GDP, and Mg^{2+}. The origin-removed cross-rotation search used data with $F > 2.0\sigma$, between 4.0 and 15.0 Å (*34*, *35*). A subsequent Patterson

correlation refinement was carried out, first refining the entire structure and then each domain separately (*36*). The top two unique peaks, with a signal-to-noise ratio (S/N) of 2.1 and 1.7, proved to be the correct solution. Translation functions were calculated using data between 4.0 and 15.0 Å (*37*). The top peak, using the Euler angles of the first cross-rotation solution, yielded a correct translation solution with a S/N of 1.1. A translation search of the second unique set of Euler angles, with and without fixing the first molecule, failed to give an obvious solution. Subsequently, the orientation of each domain for the second solution was further refined by performing a local angular search, ±30° around each Euler angle, using a direct rotation function (*38*). Using the refined Euler angles, a translation search for domain 1 of the second molecule was performed, with the first molecule fixed. The top solution, with a S/N of 1.2, ultimately proved to be the correct solution. The initial *R* factor for one copy of EF-Tu-GDP and a second copy of domain 1 was 50.2%. The whole EF-Tu model was superimposed upon domain 1 of the second translation solution and, together with the translation solution for the first molecule, was used as a starting model for rigid-body refinement.

Difference Maps and Refinement. Crystallographic refinement was carried out using X-PLOR (*33*). A random sample of 7% of the data was excluded from the refinement, and the agreement between the calculated and observed structure factors for the excluded reflections (R_{free}) was used to monitor the course of the refinement (*39*). Standard protein (*40*) and nucleotide (*41*) parameter files were used. In each rigid-body refinement calculation, 40 cycles of refinement were carried out, first on the entire EF-Tu molecule and then on each domain as a separate group. All data, with an $F > 2\sigma$, were used, initially in the resolution range of 4.0−10.0 Å and subsequently in the range of 2.4−8.0 Å. Each copy of the initial model included residues 9−393 of EF-Tu, GDP, and Mg^{2+}. Rigid-body refinement yielded an R_{work} of 40.4% and an R_{free} of 40.3%. A bulk solvent correction was applied (*42*), using a resolution range of 2.4−30.0 Å. Forty cycles of positional refinement, with the α-carbons restrained, were carried out using the same resolution range and using the suggested weight calculated by the check stage protocol. Positional refinement was continued for an additional 100 cycles, yielding an R_{work} of 32.8% and an R_{free} of 35.6%. Simulated annealing (*43*, *44*) and positional refinement, using noncrystallographic symmetry restraints, followed by individual restrained thermal-factor refinement, reduced R_{work} to 26.4% and R_{free} to 31.9%. SigmaA-weighted $2F_o - F_c$ and $F_o - F_c$ maps (*45*) were calculated, and the electron density for the antibiotic was readily apparent at 1.2σ and 2.5σ in the respective maps. Using the nuclear magnetic resonance (NMR) coordinates of GE2270A as a starting point (*46*), the antibiotic was built into the electron density using the program O (*47*). The model was visibly adjusted to improve the fit, and residues 4−8 were added to one of the two copies of EF-Tu. Parameter and topology files for GE2270A were generated with the XPLO2D program (*48*), and then parameters were adjusted until refinement of the antibiotic model alone maintained good geometry. Before each subsequent round of refinement, a new bulk solvent correction was applied and a new weight was calculated. After simulated annealing, positional, and thermal-factor refinement, R_{work} was reduced to 23.3% and R_{free} to 28.8%. Water molecules were assigned to the top peaks in the $F_o - F_c$ electron density maps if the peaks satisfied reasonable distance and geometry criteria. All subsequent refinements were carried out using a resolution range of 2.35−30.0 Å. After several alternating rounds of adding waters, followed by positional and thermal-factor refinement, the R_{work} was 20.6% and the R_{free} 26.6%. The final rounds of positional and temperature-factor refinement were carried out with the program CNS (*49*), employing the same resolution range as used in the X-PLOR refinements. The same test set and working set of reflections were maintained, except that a F/σ cutoff of 0.0 was used. The maximum likelihood target was used for refinement.

Final Model. In the asymmetric unit, the final model consists of two copies of the protein, amino acids 3−393 in chain A and 9−393 in chain B, two copies of GDP, two Mg^{2+} ions, two copies of GE2270A, 25 acetate ions, and 381 water molecules. As a consequence of weak or nonexistent electron density, the model does not include two amino acids at the N-terminus of chain A or eight amino acids at the N-terminus of chain B of EF-Tu. A sample of the SigmaA-weighted $F_o - F_c$ annealed omit map in the region of the antibiotic is shown in Figure 2. The final model has a crystallographic refinement factor of 20.6% for all measured reflections with structure-factor amplitudes $F > 0.0$ in the resolution range of 2.35−30.0 Å. The root-mean-square deviations are 0.008 Å from bond length ideality and 1.450° from bond angle ideality. The quality of the model was checked by plotting a Ramachandran map and the geometry evaluated using PROCHECK (*50*). Only two residues, Ile 247 and Arg 333, lie outside the normal range of ϕ and ψ values in the structure presented here as well as in all published EF-Tu models. The refinement statistics for the final model are summarized in Table 1.

Structural Comparisons. Structural comparison studies with EF-Tu-GDP−GE2270A and other EF-Tu complexes were carried out in O, with superpositions calculated with the lsq_explicit and lsq_improve commands, using only the residues in the GE2270A binding domain for the least-squares calculations. The EF-Tu-GDP−GE2270A complex was superimposed upon a model of *Thermus thermophilus* EF-G in a similar fashion.

RESULTS AND DISCUSSION

Antibiotic Binding Site. GE2270A is highly insoluble in water, yet as shown in Figure 2, a difference Fourier analysis produced well-ordered electron density that is unambiguously compatible with the chemical structure of GE2270A. The conformation of the bound antibiotic differs considerably from the conformation of the antibiotic in dimethyl sulfoxide as determined by NMR techniques (*46*). As shown in Figures3 and 4a, the labeled side of the antibiotic is exposed to the solvent region and the other side binds to a pocket in the second domain of EF-Tu-GDP. The pocket is formed by three segments of amino acids, Glu 215−Arg 230, Thr 256−Leu 264, and Asn 273−Leu 277. The predominant interactions between the antibiotic and the protein appear to be van der Waals interactions. There are 101 interactions between the antibiotic and the protein at a distance of ≤3.8 Å. The strongest interactions are localized to nine residues, including Arg 223, Thr 256, Gly 257, Glu 259, Phe 261, Asn 273, Val 274, Gly 275, and Leu 277, which together

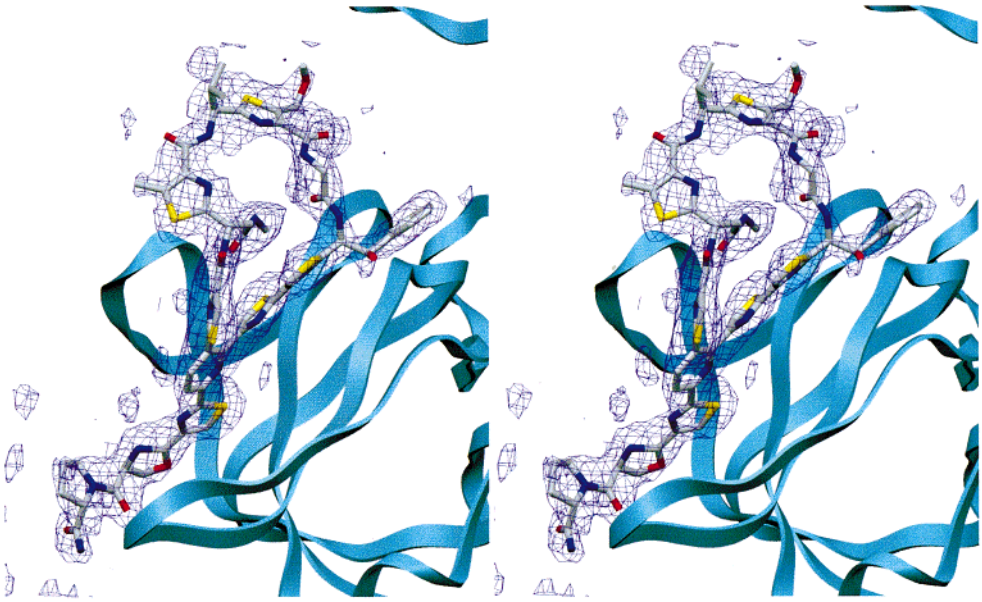

FIGURE 2: Stereoview of the electron density for GE2270A. Shown is a SigmaA-weighted $F_o - F_c$ annealed omit map, contoured at 2.3σ and superimposed with the GE2270A model shown in CPK colors, the protein backbone as a light blue ribbon, and the electron density map in purple. This figure was generated with SETOR (*56*).

Table 1: Crystal Parameters, Data Collection, and Refinement

space group	*C*2
no. of protein residues/no. of protein atoms	775/5987
no. of total reflections/no. of unique reflections	55193/31214
completeness (%)	
all data	86.9
two highest-resolution shells	60.7, 82.4
average redundancy of observations	1.8
R_{sym} (%)	3.2
molecular replacement	
crystallographic *R* factor (%)	50.2
correlation coefficient	0.46
refinement	
resolution range (Å)	2.35−30.0
no. of reflections used in the working data set/σ cutoff	29036/$F > 0.0$
no. of reflections used in the test data set/σ cutoff	2178/$F > 0.0$
no. of acetate ions	25
no. of ordered waters	381
R_{free} (%)[a]	24.9
R_{work} (%)[b]	20.2
rms deviation for bonds (Å)	0.01
rms deviation for angles (Å)	1.42
protein mean thermal factor (Å^2)	26.66
GE2270A mean thermal factor (Å^2)	39.57
MgGDP mean thermal factor (Å^2)	21.63
acetate ion thermal factor (Å^2)	51.32
waters mean thermal factor (Å^2)	38.63
all atoms (Å^2)	28.00

[a] R_{free} is the crystallographic refinement factor calculated only on the 7% of the reflections that were set aside for cross validation and not used in refinement. [b] $R_{work} = \Sigma|F_o - F_c|/\Sigma|F_o|$ for the 93% of the reflections used in the refinement calculations.

form 18 nonbonded contacts (<3.5 Å) with the antibiotic. As shown in Figure 3, there are only five hydrogen bond interactions between the antibiotic and the protein. These include GE O39 and Oδ2 of Asp 216, GE N1 and the carbonyl oxygen of Gly 222, GE N20 and NH1 of Arg 223, GE O77 and the amide nitrogen of Phe 261, and GE S70 and Nϵ of Arg 262. In addition, the antibiotic appears to be locked into the binding site by a salt bridge between NH1 of Arg 223 and Oϵ1 of Glu 259. The latter residues have a different orientation in all known EF-Tu conformations and do not interact with one another (*2*−*7*). The salt bridge is likely to account for the high stability of the antibiotic−protein complex. The two residues are not conserved in all species of EF-Tu, suggesting that the antibiotic may not bind as tightly to other bacterial forms of EF-Tu in which one of the residues is altered. The formation of the salt bridge over the antibiotic alters the surface charge in the region so as to provide a plausible explanation for the observed shift in the electrophoretic mobility of EF-Tu in native gels in the presence of GE2270A (*8*, *27*).

Mechanism of Inhibition. A superposition of the *E. coli* EF-Tu-GDP and EF-Tu-GDP−GE2270A structures reveals that the antibiotic causes only small regional changes in the side chains, but does not alter the peptide backbone significantly. This finding is consistent with biochemical studies that indicate the binding of the antibiotic to EF-Tu-GDP does not alter the dissociation rate constant, 2.3×10^4 s^{-1}, or the association rate constant, 35×10^{-4} s^{-1} M^{-1}, of GDP and the protein (*27*). If it is assumed that the antibiotic interacts with the same protein residues in all other EF-Tu conformations, the second domain of EF-Tu-GDP−GE2270A was superimposed on domain 2 from other EF-Tu conformations to ascertain the structural effects of antibiotic binding. When domain 2 of the EF-Tu-GDP−GE2270 complex is superimposed upon domain 2 of *Thermus aquaticus* EF-Tu-GTP (*7*), as shown in Figure 4b, a portion of the antibiotic occupies the same spatial location as residues 67−69, 77−79, and 98 in domain 1 of the GTP form of *T. aquaticus* EF-Tu. It is well established that the binding of GTP to EF-Tu causes a major conformational change in the GDP state, primarily shifting the relative orientation of domains 2 and 3 with respect to domain 1, the nucleotide binding domain (*6*, *7*). The superposition studies suggest that the binding of the antibiotic to domain 2 would cause a steric clash with domain 1 that effectively prevents the complete formation of the GTP conformation. The observation is also consistent with the biochemical studies. When GE2270A is added to EF-Tu-GTP, the dissociation constant for dissociation of GTP from the protein, 530 nM, decreases to 1.2 nM, a value which

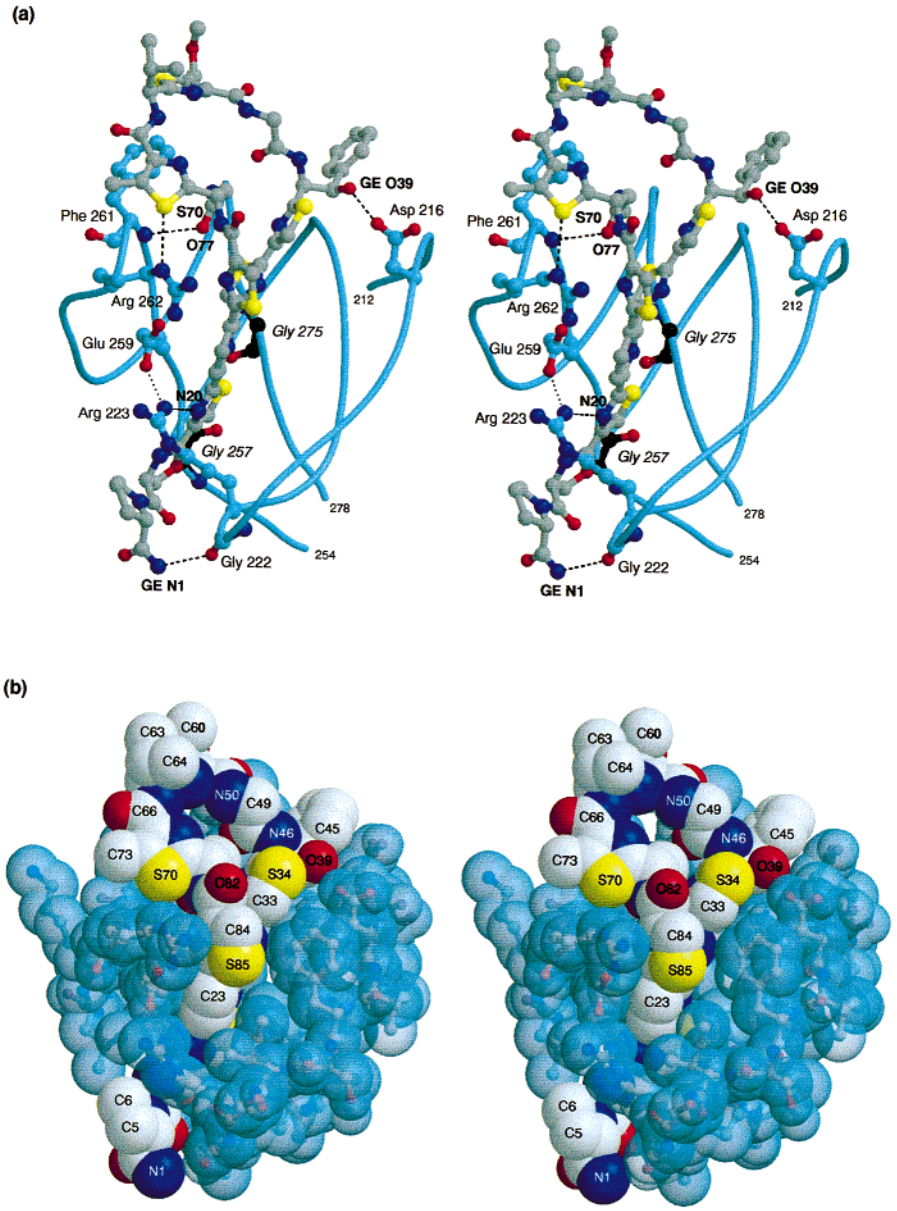

FIGURE 3: GE2270A interactions with domain 2 of *E. coli* EF-Tu-GDP. (a) Electrostatic and hydrogen bond interactions between molecule A of GE2270A and EF-Tu. GE2270A is depicted as a ball-and-stick representation, with carbon atoms shown in gray, nitrogen atoms in blue, oxygen atoms in red, and sulfur atoms in yellow. The region of EF-Tu surrounding the binding site is illustrated as light blue coils. Hydrogen bonds between EF-Tu and GE2270A are shown as dashed lines. The salt bridge, which folds over the antibiotic, is shown as a dotted line between Arg 223 and Glu 259. GE2270A resistance in other bacteria is conferred by mutation at sites equivalent to Gly 257 and Gly 275, whose carbon atoms are shown in black. (b) van der Waals interactions between GE2270A and EF-Tu. The orientation is the same as that shown in panel a. GE2270A is represented by solid van der Waals spheres, with carbon atoms colored in gray, nitrogen atoms in blue, oxygen atoms in red, and sulfur atoms in yellow. Selective atomic labels are included on the van der Waals spheres for the antibiotic. EF-Tu residues 212−231, 255−265, and 271−278 are shown as ball-and-stick representations, with transparent blue van der Waals spheres enclosing the atoms. The close fit of the antibiotic into a groove in the protein is illustrated. Also visible is the salt bridge between Arg 223 and Glu 259 that folds over the noncyclic end of the antibiotic. Both parts of this figure were generated using MOLSCRIPT (*57*) and Raster3D (*58*).

is more similar to 0.7 nM, the dissociation constant for dissociation of GDP from EF-Tu (*27*). Domain 2 of the EF-Tu-GDP−GE2270A complex has also been superimposed upon the *T. aquaticus* EF-Tu−phenylalanyl-tRNA complex (*5*) as shown in Figure 4c. In addition to the steric clash between the antibiotic and domain 1 of the GTP form already noted, portions of GE2270 occupy the same binding site as the aminoacyl group of the tRNA. This finding is also consistent with the biochemical studies that demonstrate that, in the presence of GE2270A, the EF-Tu-GTP−aminoacyl-tRNA complex is not formed (*8*, *9*, *27*). Altogether, the superposition studies suggest that two distinct regions of GE2270A inhibit the function of EF-Tu, one by blocking the complete conformational rearrangement to the GTP conformation and the second by preventing the binding of aminoacyl-tRNA.

Mechanism of Antibiotic Resistance. The structural results for the EF-Tu-GDP−GE2270A complex explain the effects of most amino acid sequence changes that confer antibiotic resistance upon an organism. Prior to structural analysis,

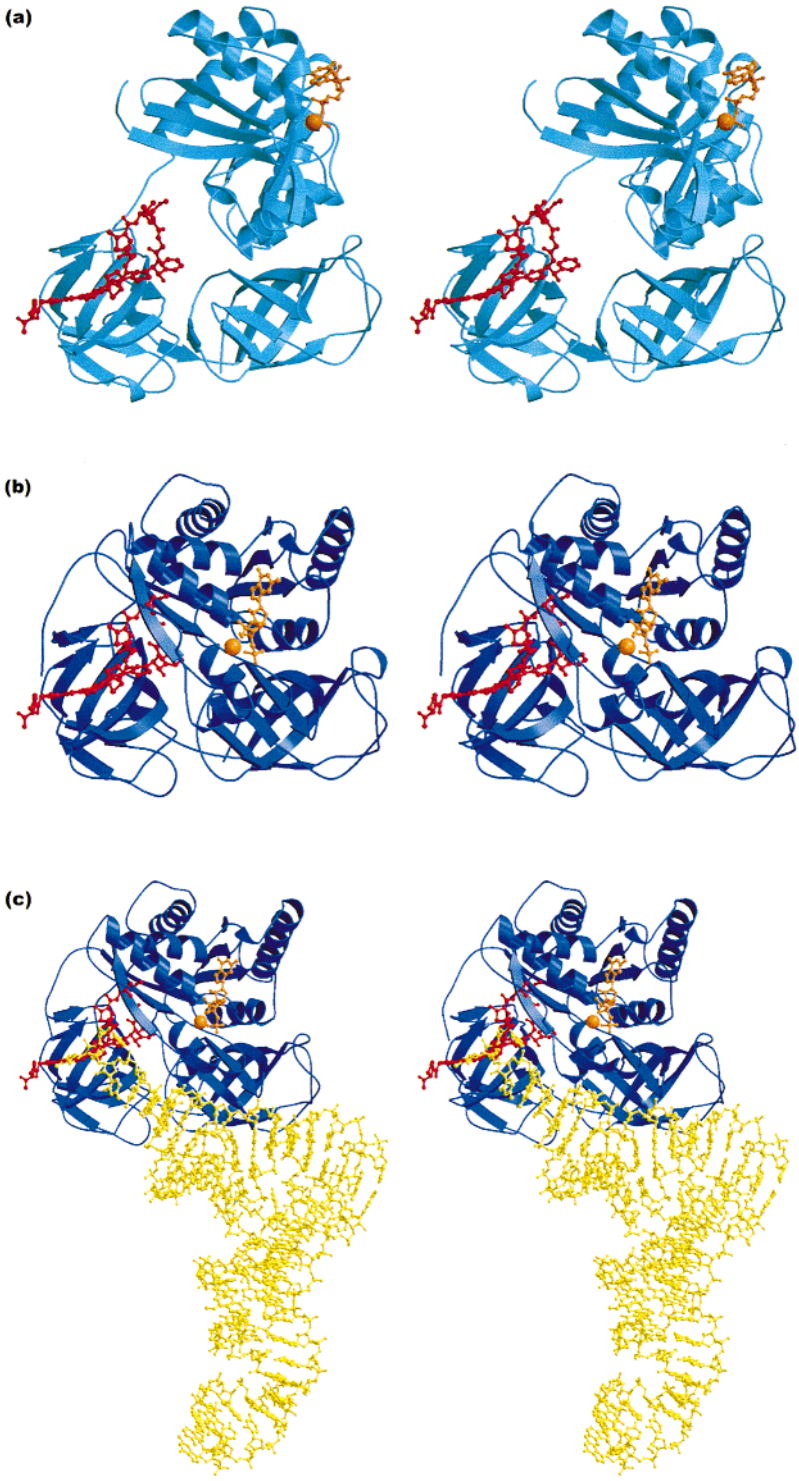

FIGURE 4: Stereoimages of GE2270A interactions with various EF-Tu conformations. In all the parts of this figure, GE2270A and GDP are shown as a ball-and-stick representation, with the antibiotic in red and GDP in orange. The Mg^{2+} ion is shown as an orange sphere. (a) Structural results of the GE2270A interaction with EF-Tu-GDP. The polypeptide backbone of EF-Tu-GDP is illustrated as a light blue ribbon image. The antibiotic binds in a pocket formed within domain 2 of EF-Tu-GDP. (b) Model of the GE2270A interaction with EF-Tu-GTP. Potential GE2270A interactions with an EF-Tu-GTP conformation have been modeled by superimposing the second domain of the EF-Tu-GDP−GE2270A structure upon the second domain of the *T. aquaticus* EF-Tu-GDPNP structure (PDB file 1EFT) shown as a dark blue ribbon. GE2270A appears to form a steric clash with residues 67−69 and 77−79 in domain 1 of the GTP conformation of *T. aquaticus* EF-Tu. (c) Model of the GE2270A interaction with EF-Tu−aminoacyl-tRNA. Potential GE2270A interactions with an EF-Tu-GTP−aminoacyl-tRNA complex have been modeled by superimposing the second domain of the EF-Tu-GDP−GE2270A complex upon the second domain of *T. aquaticus* EF-Tu-GDPNP in complex with yeast phenylalanine-tRNA (PDB file 1TTT; chains A and D). *T. aquaticus* EF-Tu is shown as a dark blue ribbon and yeast phenylalanine-tRNA as a gold ball-and-stick model (PDB file 1TTT; chains A and D). GE2270A occupies the same spatial location as the aminoacyl group. All three parts of this figure were generated using MOLSCRIPT (*57*) and Raster3D (*58*).

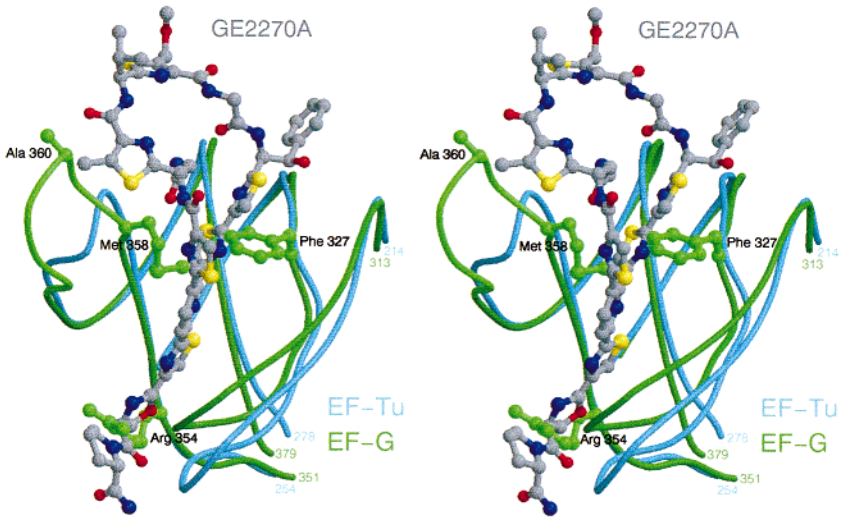

FIGURE 5: Stereoimage of the model of GE2270A interactions with domain 2 of *T. thermophilus* EF-G-GDP. Potential GE2270A interactions with EF-G-GDP have been modeled by superimposing the second domain of the EF-Tu-GDP−GE2270A structure upon the second domain of the *T. thermophilus* EF-G-GDP structure (PDB file 1DAR). The region encompassing the antibiotic binding site is shown in light blue for EF-Tu-GDP and in green for EF-G-GDP. GE2270A is depicted as a ball-and-stick representation, with carbon atoms shown in gray, nitrogen atoms in blue, oxygen atoms in red, and sulfur atoms in yellow. The orientation is the same as that shown in Figure 3a. There are several EF-G regions that appear to have a steric clash with GE2270A, including the side chain atoms of Phe 327, Arg 354, and Met 358 and the main chain atoms of His 359 and Ala 360. This figure was generated using MOLSCRIPT (*57*) and Raster3D (*58*).

several groups had attempted to map the GE2270A or the amythiamicin D binding site by identifying *B. subtilis* mutants that are resistant to the antibiotics. In one report, a G278S mutation in *B. subtilis* EF-Tu conferred resistance to GE2270A (*23*). *B. subtilis* Gly 278 is equivalent to *E. coli* Gly 275 which makes six strong van der Waals and hydrogen bonding interactions with the antibiotic. The structural results suggest that a mutation from glycine to any other residue would cause a steric problem, preventing close antibiotic interactions, not only with a residue at the Gly 275 position but also with other amino acids in the binding pocket. Another site-specific EF-Tu mutation in *B. subtilis*, known to induce resistance to a related antibiotic, amythiamicin D, is V228A (*26*). The equivalent site in *E. coli* is Val 226. Only the penultimate carbon atoms of the Val 226 make van der Waals contacts with the antibiotic. A substitution from valine to alanine would eliminate all of the van der Waals interactions and create a "hole", but would not obviously affect other interactions between the protein and the antibiotic. Thus, it is somewhat difficult to understand why this substitution so strongly disrupts the binding of GE2270A to the mutant EF-Tu. It has also been demonstrated that the organism, *P. rosea*, which produces GE2270A naturally, has two *tuf* genes, each of which encodes an EF-Tu that is resistant to the antibiotic (*23*, *24*). In the *tuf1* gene product of *P. rosea*, there are six amino acid differences with *E. coli* EF-Tu in the GE2270A binding pocket, including Ser 261, Ile 262, Asn 266, Met 268, Ala 278, and Ala 279. In *E. coli*, these residues correspond to Gly 257, Val 258, Arg 262, Leu 264, Val 274, and Gly 275, respectively. Like Gly 275 discussed previously, Gly 257 makes five strong van der Waals contacts with the antibiotic. A substitution from glycine to any other amino acid is likely to cause a steric problem, preventing close interactions between the antibiotic and many sites on the protein. The side chain of Arg 262 makes one hydrogen bond and five van der Waals contacts with the antibiotic. A substitution from arginine to asparagine, as found in *P. rosea*, would preserve the hydrogen bond but eliminate the van der Waals interactions. However, a more radical substitution, such as to histidine and glycine, as observed in EF-Tu from *Micrococcus luteus* (*51*) and *Streptomyces coelicolor* (*52*), respectively, might prove to be more disruptive to antibiotic binding. In the Leu 264 interaction, a weak van der Waals contact is observed. A substitution to methionine, as observed in *P. rosea*, would likely disrupt the contact but may form others. Val 258 and Val 274 form contacts with the antibiotic only through the backbone atoms, with the side chains oriented away from the antibiotic. Thus, a substitution to isoleucine or valine, as found in *P. rosea*, would not likely disrupt antibiotic binding. Given the preceding analysis, the amino acid substitutions most likely to cause antibiotic resistance are Ser 261 and Ala 279 in *P. rosea*. A mutation in an equivalent position in a mutant strain of *B. subtilis*, G278S in *B. subtilis* nomenclature, was also found to cause GE2270A resistance (*23*).

Specificity for EF-Tu. Biochemical studies indicate that GE2270A acts specifically upon EF-Tu, and not upon other ribosomal GTPases, including the translocation factor, EF-G, which is similar in sequence and structure to domains 1 and 2 of EF-Tu. To determine if GE2270A might also inhibit EF-G, the second domain of the EF-Tu-GDP−GE2270A complex was superimposed upon the second domain of *T. thermophilus* EF-G-GDP (*53*), as shown in Figure 5. From the comparison, it appears GE2270A would cause a steric clash with five conserved amino acids of EF-G, including residues Phe 327, Arg 354, Met 358, His 359, and Ala 360. The latter two amino acids are found in a highly conserved loop in EF-G, but one that is not present in EF-Tu. A similar question has been asked of the eukaryotic elongation factor, EF-1α. Although a structure of a eukaryotic EF-1α is not available, an analysis of the multiple sequence alignment of prokaryotic and eukaryotic elongation factors available in ProDom (*54*) reveals a clear difference. Two conserved prokaryotic residues, critical to the interaction with GE2270A, are different and invariant in the eukaryotic elongation

factors. Arg 223 in *E. coli* EF-Tu, which is involved in formation of the salt bridge over the antibiotic, is equivalent to Ile 259 in human EF-1α, a residue that is invariant among the eukaryotic EF-1α family. Gly 257 in *E. coli* EF-Tu, which allows close contact with the antibiotic, is equivalent to the conserved Ser/Thr 291 in the eukaryotic EF-1α family. Thus, it is highly unlikely that GE2270A could bind to eukaryotic elongation factors. The final question of interest is the similarity between GE2270A and thiostrepton, a well-characterized member of the cyclic thiazolyl peptide antibiotic class. Thiostrepton is reported to bind to a region of 23S rRNA spanning residues 1052−1112, blocking the binding of EF-G to the ribosome (*22*). Thiostrepton is not reported to bind directly with any of the ribosomal GTPases, including EF-Tu and EF-G. Although the structure of thiostrepton has been determined **(***55*), the atomic coordinates are unavailable and a rigorous atomic comparison is not possible. Nevertheless, a comparison of the chemical structures of GE2270A and thiostrepton reveals that the extra cyclic ring of thiostrepton would not likely interfere sterically with a putative interaction with the protein. Instead, it appears that the geometry around C24, which is tetrahedral in thiostrepton but planar in GE2270A, is most likely to alter the shape of the antibiotic, such that the complementary fit of GE2270A into a groove in EF-Tu would be disrupted.

Summary. The three-dimensional structure of the EF-Tu-GDP−GE2270A complex provides atomic details of the antibiotic site on the protein and reveals the regions of the antibiotic that are solvent-accessible sites, perhaps useful for chemical modifications for improving the aqueous solubility of the natural compound. The structure also provides a rational explanation for the mode of antibiotic inhibition as well as the observed resistance that has occurred through sequence-specific changes in EF-Tu.

ACKNOWLEDGMENT

We gratefully acknowledge Enrico Selva and Khalid Islaam of Biosearch Italia for a gift of GE2270A and the NMR coordinates of GE2270A. We also gratefully acknowledge the assistance of Annette Arora, Steven Herron, and Stephan Watkins in the preparation of the manuscript. The research was conducted, in part, at Stanford Synchrotron Radiation Laboratory which is operated by the Office of Basic Energy Science of the U.S. Department of Energy.

REFERENCES

1. Abel, K., and Jurnak, F. (1996) *Structure 4*, 229−238.
2. Abel, K., Yoder, M. D., Hilgenfeld, R., and Jurnak, F. (1996) *Structure 4*, 1153−1159.
3. Polekhina, G., Thirup, S., Kjeldgaard, M., Nissen, P., Lippmann, C., and Nyborg, J. (1996) *Structure 4*, 1141−1151.
4. Kawashima, T., Berthet-Colominas, C., Wulff, M., Cusack, S., and Leberman, R. (1996) *Nature 379*, 511−518.
5. Nissen, P., Kjeldgaard, M., Thirup, S., Polekhina, G., Reshetnikova, L., Clark, B. F., and Nyborg, J. (1995) *Science 270*, 1464−1472.
6. Berchtold, H., Reshetnikova, L., Reiser, C. O., Schirmer, N. K., Sprinzl, M., and Hilgenfeld, R. (1993) *Nature 365*, 126−132.
7. Kjeldgaard, M., Nissen, P., Thirup, S., and Nyborg, J. (1993) *Structure 1*, 35−50.
8. Anborgh, P. H., and Parmeggiani, A. (1991) *EMBO J. 10*, 779−784.
9. Landini, P., Bandera, M., Goldstein, B. P., Ripamonti, F., Soffientini, A., Islam, K., and Denaro, M. (1992) *Biochem. J. 283*, 649−652.
10. Shimanaka, K., Kinoshita, N., Iinuma, H., Hamada, M., and Takeuchi, T. (1994) *J. Antibiot. 47*, 668−674.
11. Parmeggiani, A., and Swart, G. W. M. (1985) *Annu. Rev. Microbiol. 39*, 557−577.
12. Wolf, H., Chinali, G., and Parmeggiani, A. (1977) *Eur. J. Biochem. 75*, 67−75.
13. Pingoud, A., Block, W., Urbanke, C., and Wolf, H. (1982) *Eur. J. Biochem. 78*, 403−409.
14. Cetin, R., Krab, I. M., Anborgh, P. H., Cool, R. H., Watanabe, T., Sugiyama, T., Izake, K., and Parmeggiani, A. (1996) *EMBO J. 15*, 2604−2611.
15. Selva, E., Beretta, G., Montanini, N., Saddler, G. S., Gastaldo, L., Ferrari, P., Lorenzetti, R., Landini, P., Ripamonti, F., Goldstein, B. P., Berti, M., Montanaro, L., and Denaro, M. (1991) *J. Antibiot. 44*, 693−701.
16. Stella, S., Montanini, N., LeMonnier, F., Ferrari, P., Colombo, L., Landini, P., Ciciliato, I., Goldstein, B. P., Selva, E., and Denaro, M. (1995) *J. Antibiot. 48*, 780−786.
17. Gale, E. F., Cundliffe, E., Reynolds, P. E., Richmond, M. H., and Waring, M. J. (1981) in *The Molecular Basis of Antibiotic Action*, pp 492−500, John Wiley & Sons, London.
18. Cundliffe, E., and Thompson, J. (1981) *J. Gen. Microbiol. 126*, 185−192.
19. Cundliffe, E., and Thompson, J. (1981) *Eur. J. Biochem. 118*, 47−52.
20. Vazquez, D. (1979) *Mol. Biol., Biochem. Biophys. 30*, 1−312.
21. Cundliffe, E. (1989) *Annu. Rev. Microbiol. 43*, 207−233.
22. Cundliffe, E. (1978) *Nature 272*, 792−795.
23. Sosia, M., Amati, G., Cappellano, C., Sarubbi, E., Monti, F., and Donadio, S. (1996) *Mol. Microbiol. 22*, 43−51.
24. Möhrle, V. G., Tieleman, L. N., and Kraal, B. (1997) *Biochem. Biophys. Res. Commun. 230*, 320−326.
25. Goldstein, B. P., Berti, M., Ripamonti, R., Resconi, A., Scotti, R., and Denaro, M. (1993) *Antimicrob. Agents Chemother. 37*, 741−745.
26. Shimanaka, K., Iinuma, H., and Hamada, M. (1995) *J. Antibiot. 48*, 182−184.
27. Anborgh, P. H., and Parmeggiani, A. (1993) *J. Biol. Chem. 268*, 24622−24628.
28. Louie, A., Ribeiro, N. S., Reid, B. R., and Jurnak, F. (1984) *J. Biol. Chem. 259*, 5010−5016.
29. Kabsch, W. (1993) *J. Appl. Crystallogr. 24*, 795−800.
30. Campbell, J. W. (1995) *J. Appl. Crystallogr. 28*, 236−242.
31. Evans, P. R. (1997) *Joint CCP4 and ESF-EACBM Newsletter 33*, 22−24.
32. French, G. S., and Wilson, K. S. (1978) *Acta Crystallogr. A34*, 517−525.
33. Brünger, A. T. (1992) *X-PLOR*, version 3.1, Yale University Press, New Haven, CT.
34. Huber, R. (1965) *Acta Crystallogr. A19*, 353−356.
35. Steigemann, W. (1974) Ph.D. Thesis, Technische Universitaet Muenchen, Muenchen, Germany.
36. Brünger, A. T. (1990) *Acta Crystallogr. A46*, 46−57.
37. Fujinaga, M., and Read, R. J. (1987) *J. Appl. Crystallogr. 20*, 517−521.
38. DeLano, W. L., and Brünger, A. T. (1995) *Acta Crystallogr. D51*, 740−748.
39. Brünger, A. T. (1992) *Nature 355*, 472−474.
40. Engh, R. A., and Huber, R. (1991) *Acta Crystallogr. A47*, 392−400.
41. Parkinson, G., Vojtechovsky, J., Clowney, L., Brünger, A. T., and Berman, H. M. (1996) *Acta Crystallogr. D552*, 57−64.
42. Jiang, J.-S., and Brünger, A. T. (1994) *J. Mol. Biol. 243*, 100−115.
43. Brünger, A. T., Kuriyan, J., and Karplus, M. (1987) *Science 235*, 458−460.
44. Brünger, A. T., Krukowski, A., and Erickson, J. (1990) *Acta Crystallogr. A46*, 585−593.
45. Read, R. J. (1986) *Acta Crystallogr. A42*, 140−149.

46. Kettenring, J., Colombo, L., Ferrari, P., Tavecchia, P., Nebuloni, M., Vékey, K., Gallo, G. G., and Selva, E. (1991) *J. Antibiot. 44*, 702−715.
47. Jones, T. A., Zou, J. Y., Cowan, S. W., and Kjeldgaard, M. (1991) *Acta Crystallogr. A47*, 110−119.
48. Kleywegt, G. J. (1995) *CCP4/ESF-EACBM Newsletter on Protein Crystallography 31*, 45−50.
49. Brònger, A. T., Adams, P. D., Clore, G. M., Delano, W. L., Gros, P., Grosse-Kunstleve, R. W., Jiang, J.-S., Kuszewski, J., Nilges, N., Pannu, N. S., Read, R. J., Rice, L. M., Simonson, T., and Warren, G. L. (1998) *Acta Crystallogr. D54*, 905−921.
50. Laskowski, R. A., MacArthur, M. W., Moss, D. S., and Thornton, J. M. (1993) *J. Appl. Crystallogr. 26*, 283−291.
51. Ohama, T., Yamao, F., Muto, A., and Osawa, S. (1987) *J. Bacteriol. 169*, 4770−4777.
52. Van Wezel, G. P., Woudt, L. P., Vervenne, R., Verdurmen, M. L., Vijgenboom, E., and Bosch, L. (1994) *Biochim. Biophys. Acta 1219*, 543−547.
53. Alkaradaghi, S., Evarsson, A., Garger, M., Zheltonosova, J., and Liljas, A. (1996) *Structure 4*, 555−565.
54. Corpet, F., Gouzy, J., and Kahn, D. (1999) *Nucleic Acids Res. 27*, 263−267.
55. Anderson, B., Hodgkin, D. C., and Viswamitra, M. A. (1970) *Nature 225*, 233−235.
56. Evans, S. V. (1993) *J. Mol. Graphics 11*, 134−138.
57. Kraulis, P. J. (1991) *J. Appl. Crystallogr. 24*, 946−950.
58. Merritt, E. A., and Bacon, D. J. (1997) *Methods Enzymol. 277*, 505−542.

BI9913597